Publ. Astron. Soc. Aust., 1999, 16, 225–33

Magnetic Fields in Accretion Disks*

Marthijn de Kool[1], Geoffrey V. Bicknell[1] and Zdenka Kuncic[2]

[1]Astrophysical Theory Centre, Research School of Astronomy and Astrophysics, Private Bag, Weston Creek, ACT 2611, Australia
[2]Department of Physics and Astronomy, University of Victoria, Box 3055, Victoria, BC V8W 3P6, Canada

Received 1999 May 20, accepted 1999 August 31

Abstract: This paper summarises our work on the role of magnetic fields in accretion disks presented in two papers elsewhere. In the first part (a summary of part of Kuncic & Bicknell 1999), we present a formal development of the equations governing the structure of an accretion disk containing magnetohydrodynamic turbulence. The importance of the different terms in the energy and momentum equations is discussed, and a parametrisation of the unresolved processes is suggested that could be used to make further progress. We briefly explore whether an MHD accretion disk can transport a significant part of the gravitational power into a corona by buoyancy. In the second part, we present some exploratory calculations of the vertical structure of accretion disks, in which non-local dissipation of energy due to the buoyant transport of magnetic field energy is taken into account. It is argued that the efficiency of buoyant magnetic transport depends very strongly on the size of the coherent magnetic regions. If the size of the buoyant cells is not very close to the disk thickness, magnetic energy generated by dynamo action inside the disk will be dissipated locally, and will not be available to transport a significant part of the accretion luminosity into a corona.

Keywords: accretion, accretion disks — magnetic fields

1 Structure Equations of MHD Accretion Disks

There are several reasons why magnetic fields are thought to play an important role in accretion disks. It is the only source of viscosity that can be derived from first principles that comes close to being effective enough to explain the high viscosity observed for accretion disks. The existence of highly collimated jets in many disk accreting astronomical objects is most easily explained if they are driven by strong magnetic fields associated with the innermost disk. More recently, very hot accretion disk corona in which a significant part of the accretion luminosity is dissipated have been observed. This has led to many suggestions that the corona is heated by a reconnecting magnetic field rising buoyantly from a cold accretion disk. Further development of this magnetically heated corona model is the main motivation for our work presented here. In this first section, we present a summary of recent work (Kuncic & Bicknell 1999) and the reader is referred there for a complete analysis of the structure of turbulent magnetised disks.

The fundamental physical idea is that an accretion disk corona is formed in a similar fashion to the solar corona: by buoyant flux of the magnetic field and subsequent magnetic heating. Some support for the picture of intense local dissipation when flux tubes reconnect comes from the work of Haardt & Maraschi (1997), who showed that the coronal X-ray emission is best modelled if the corona is patchy. The magnetic field is generated in the accretion disk by dynamo action, at a rate of the same order as the gravitational power. If the magnetic fields in the accretion disk are responsible for the viscosity, they must be quite strong, roughly in equipartition with the gas pressure. Such a strong magnetic field will be buoyant, and will be transported to several disk scale heights before dissipating by reconnection in the high Alfvén speed environment of the corona (Galeev, Rosner & Vaiana 1979; Tout & Pringle 1992). Note that magnetic heating of the corona is not the only possibility: the standard viscous heating assumption ($H \propto \alpha P$) used in the Shakura & Sunyaev (1973) accretion disk models can also lead to hot outer disk layers, since cooling in the low density environment is not very effective (Shaviv & Wehrse 1986; Meyer & Meyer-Hofmeister 1994). However, in these models most of the luminosity is

*Refereed paper based on two separate contributions to the Workshop on Magnetic Fields and Accretion, held at the Astrophysical Theory Centre, Australian National University, on 12–13 November 1998.

 1323-3580/99/030225$05.00

still generated in the cold part of the disk where the pressure is high.

In the remainder of this section a careful development of the thin disk equations will be presented, with a turbulent magnetic field included. The formalism will include the possible effects of a disk wind and buoyancy, and will lead to an estimate of the buoyant Poynting flux in terms of the disk parameters.

1.1 Disk Equations

In analogy with the Shakura–Sunyaev disk theory, we formulate vertically averaged thin disk equations by integrating the MHD equations between $z = h$ and $z = -h$, where in our case h is the height of the disk–corona boundary. The surface density Σ and average disk height h_{av} are defined by

$$\Sigma = \int_{-h}^{h} \rho dz \equiv 2\overline{\rho} h\,, \tag{1}$$

$$h_{av} = \frac{2}{\Sigma}\int_{0}^{h} \rho z dz\,. \tag{2}$$

The mass flux in the disk wind and the mass flux through the disk are defined as

$$\dot{M}_w(r) = 4\pi \int_{r_0}^{r} \rho^+ \; v_z^+ \; r \; dr, \tag{3}$$

$$\dot{M}_a(r) = \dot{M}_a(r_0) \;\; + \;\; \dot{M}_w(r), \tag{4}$$

where r_0 is the innermost stable orbit, and the superscript + refers to conditions at the disk–corona boundary.

The radial momentum balance is described by the equation

$$\Sigma\left(\frac{v_\phi^2}{r} - \frac{GM}{r^2}\right) + \frac{\langle B_r B_z\rangle}{4\pi}\Big|_{-h}^{h} = 0, \tag{5}$$

which leads to the expression for the azimuthal velocity

$$v_\phi^2 = v_K^2 - \frac{2r\langle B_r^+ B_z^+\rangle}{4\pi\Sigma}, \tag{6}$$

where $v_K = (GM/R)^{\frac{1}{2}}$ is the local Keplerian velocity. The second term on the RHS of this equation represents the radial force due to the magnetic tension along field lines penetrating the disk surface. If the magnetic field strength is not significantly above equipartition, this term can be shown to be $\lesssim (h/r)v_K^2$ so that the rotation is still close to Keplerian.

For the vertical momentum balance we ignore the dynamical terms, and obtain

$$\frac{\partial P_g}{\partial z} + \frac{\partial}{\partial z}\left(\frac{\langle B_r^2 + B_\phi^2 - B_z^2\rangle}{8\pi}\right) - \frac{1}{4\pi r}\frac{\partial}{\partial r}\left(r\langle B_r B_z\rangle\right) + \frac{GM}{r^3}\rho z = 0\,. \tag{7}$$

Integrating this equation from $z = 0$ to $z = h$ yields

$$P_g(r,0) + \frac{\langle B_r^2 + B_\phi^2 - B_z^2\rangle}{8\pi}(r,0) = \tfrac{1}{2}\frac{GM}{r^3}\Sigma h_{av}, \tag{8}$$

where $h_{av} = \int_0^h \rho z\, dz / \int_0^h \rho\, dz$ is an average scale height based upon the profile of the mean density. Because of the strong shearing we expect B_ϕ to dominate the magnetic energy density, and to a good approximation $P_{tot} = P_g + B_\phi^2/8\pi$. For an approximately isothermal disk we have

$$(P, \rho) = (P_0, \rho_0)\exp(-z^2/h_s^2), \tag{9}$$

where P_0 and ρ_0 are the central pressure and density, respectively, and h_s is the scale-height. We use this to approximately relate h_{av} and h_s, thus, $h_s = \sqrt{\pi} h_{av}$. The following theory does not depend strongly upon this relationship; it simply improves upon the obvious order of magnitude relationship $h_s \sim h_{av}$.

Using this relationship between h_s and h_{av}, together with $\Sigma(r) \approx \sqrt{\pi}\rho_0 h_s$, and taking v_s as the isothermal sound speed, we can solve equation (8) for the scale-height:

$$\frac{h_s}{r} = \sqrt{2}\frac{v_s}{v_K}\left[1 + \frac{B^2}{8\pi P_0}\right]^{\frac{1}{2}}. \tag{10}$$

The angular momentum transport through the disk is described by the vertically averaged ϕ component of the momentum equation

$$\frac{d}{dr}[\dot{M}_a r v_\phi + r^2 h(r)\langle\overline{B_r B_\phi}\rangle - 4\pi r^2 h(r)\langle\overline{\rho v_r' v\phi'}\rangle] = 4\pi r\rho^+ v_\phi^+ v_z^+ - r^2\frac{\langle B_\phi B_z\rangle}{2}\Big|_{-h}^{h}. \tag{11}$$

The first term on the RHS represents angular momentum loss from the disk surface due to a wind, the second term angular momentum loss due to tension along magnetic field lines crossing the surface. If there is no angular momentum loss from the surface the RHS of this equation is zero, and we derive the following expression for the total averaged

https://doi.org/10.1071/AS99225 Published online by Cambridge University Press

turbulent stress $\overline{\tau}_{r\phi}$, which is composed of magnetic and hydrodynamic turbulent contributions:

$$\overline{\tau}_{r\phi} = \frac{\langle \overline{B_r B_\phi} \rangle}{4\pi} - \langle \overline{\rho v_r' v_\phi'} \rangle = \frac{\dot{M}_a v_\phi}{4\pi r h}[1 - \zeta(r)] \,. \qquad (12)$$

Here $\zeta(r)$ is set by the boundary condition specifying the stress at r_0. For the usual assumption of vanishing stress at $r = r_0$, we have $\zeta(r) = \sqrt{r_0/r}$.

Shearing box studies of MHD turbulence in accretion disks (Stone et al. 1996) have shown that the hydrodynamic and magnetic stresses are comparable. Therefore, it is convenient to parametrise these stresses in the following way:

$$\langle \overline{\rho v_r' v_\phi'} \rangle = -(1 - \eta)\overline{\tau}_{r\phi} \,, \qquad (13)$$

$$\frac{\langle \overline{B_r B_\phi} \rangle}{4\pi} = \eta \overline{\tau}_{r\phi} \,, \qquad (14)$$

with $\eta \sim 0{\cdot}5$. To make the connection with non-magnetic standard α-disk models, we parametrise the total stress in term of the gas pressure P_g:

$$\langle \overline{\rho v_r' v_\phi'} \rangle = \alpha \overline{P}_g \,. \qquad (15)$$

As in standard Shakura–Sunyaev disks, we expect $\alpha \lesssim 1$.

We now turn to the energy equations. The overall disk energy balance is expressed by

$$\begin{aligned} L_D &= \int_{r_0}^{r} 4\pi r \sigma T_{eff}^4 dr \\ &= \frac{GM\dot{M}_a(r_0)}{2r_0} - \int_{r_0}^{\infty} \frac{GM}{2r} d\dot{M}_w \\ &\quad - \int_{r_0}^{\infty} 2\pi r \left[2v_z^+ \frac{\langle B_\phi^2 \rangle}{8\pi} \right. \\ &\quad \left. - 2v_\phi \frac{\langle B_\phi^+ B_z^+ \rangle}{4\pi} \right] dr + \xi L_c + L_Q \,. \end{aligned} \qquad (16)$$

The terms on the RHS have the following physical meaning: the first one is the standard disk luminosity; the second represents gravitational potential energy lost in a wind; the next two magnetic terms are the Poynting flux lost in the wind and the work done against the disk by magnetic tension; and the last two terms are the fraction ξ of the coronal luminosity L_c that is absorbed by the disk and the conductive energy flux from corona into the disk L_Q.

The full energy equation contains many processes that we do not fully understand. It is therefore convenient to parametrise them in terms of the total available gravitational power,

$$P_G = \frac{GM\dot{M}_a(r_0)}{2r_0} \,. \qquad (17)$$

We write the luminosity of the disk as

$$L_D = (1 - f_w - f_B)P_G + \xi L_c + L_Q \,. \qquad (18)$$

If all the energy lost from the disk through the magnetic terms is used to heat the corona, we have

$$L_c = (1 - q_c) f_B P_G \,, \qquad (19)$$

$$L_Q = q_c f_B P_G, \qquad (20)$$

where q_c is the fraction of the coronal power that is conducted back into the disk.

High energy (∼100 keV) spectra of Seyfert galaxies can generally be fitted successfully with a thermally Comptonised spectrum with a typical temperature and optical depth of the scattering gas of $T \sim 10^9$ K and $\tau_{es} \sim 1$, or a Compton y-parameter of order 1. Using the parametrisation above, we find

$$\begin{aligned} e^y - 1 &= \frac{L_c}{L_D} \\ &= \frac{(1 - q_c) f_B}{1 - f_w - f_B[1 - \xi(1 - q_c) - q_c]} \,. \end{aligned} \qquad (21)$$

Most disk corona models do not take all possible effects into account; for example, Haardt & Maraschi (1997) assumed $f_w = q_c = 0$.

1.2 Magnetic Field Evolution

To describe the evolution of the turbulent magnetic field in the accretion disk, we start with the general induction equation

$$\frac{\partial \mathbf{B}}{\partial t} + \mathrm{curl}(\mathbf{B} \times \mathbf{v}) = \frac{c^2}{4\pi\sigma} \nabla^2 \mathbf{B} \,. \qquad (22)$$

From this we can derive the equation describing the generation of magnetic energy density ϵ_B:

$$\begin{aligned} &\frac{\partial \epsilon_B}{\partial t} + \frac{\partial}{\partial x_j}(\epsilon_B v_j) + \tfrac{1}{3}\epsilon_B v_{j,j} \\ &\qquad = \frac{B_i B_j}{4\pi} s_{ij} + \text{dissipation terms} \,. \end{aligned} \qquad (23)$$

https://doi.org/10.1071/AS99225 Published online by Cambridge University Press

Here s_{ij} is the shear tensor; $s_{ij} = \frac{1}{2}\left[v_{i,j} + v_{j,i} - \frac{2}{3}v_{k,k}\delta_{ij}\right]$. This identifies a mean volume rate of generation of magnetic energy density, given by

$$\dot{\epsilon}_B = \frac{\langle B_i B_j \rangle}{4\pi}\langle s_{ij}\rangle \approx \frac{3\langle B_r B_\phi\rangle}{8\pi}\Omega$$

$$= \tfrac{3}{2}\eta\tau_{r\phi}\Omega = \frac{3\eta G M \dot{M}_{\rm a}}{8\pi r^3}\left[1-\zeta(r)\right], \qquad (24)$$

where we have used the expression for the stress in terms of the mass accretion rate (equation 12). Thus, for significant values of η, the rate of magnetic energy generation is comparable to the gravitational power. Galeev, Rosner & Vaiana (1979) have argued that this energy is mostly dissipated in a corona because dissipation inside the disk is negligible as a result of the low Alfvén speed (see also the next section).

Similarly, the rate of generation of turbulent kinetic energy is given by

$$\dot{\epsilon}_{TKE} = -\langle \rho v_i' v_j'\rangle\langle s_{ij}\rangle = \tfrac{3}{2}(1-\eta)\tau_{r\phi}\Omega$$

$$= \frac{3(1-\eta)GM\dot{M}_{\rm a}}{8\pi r^3}\left[1-\zeta(r)\right], \qquad (25)$$

and this reduces to the standard, unmagnetised disk expression when $\eta = 0$. We emphasise that neither of these expressions directly gives the rate of *dissipation* of energy as is conventionally assumed in accretion disk theory. This involves another step, either dissipation at the dissipative scale of a turbulent cascade or dissipation resulting from reconnection of transported energy, or both.

1.3 Poynting Flux resulting from Buoyancy

In order to estimate the power that may be dissipated in the corona, we extend the above theory to consider the buoyant transport of a magnetic field in a disk. We balance the drag force on a flux tube of diameter D, located a height z above the central plane of the disk and with stronger than average magnetic field, with the buoyancy force in the following way:

$$C_D\,\rho v_b^2\,D \approx \left(\frac{\delta\rho}{\rho}\right)\left(-\frac{\partial P}{\partial z}\right)\frac{\pi D^2}{4}, \qquad (26)$$

where C_D is the drag coefficient and v_b is the buoyant velocity. This gives

$$\Rightarrow v_{\rm b} \approx \left(\frac{\pi}{4}\right)^{\frac{1}{2}} C_D^{-1/2}\left(\frac{\delta\rho}{\rho}\right)^{\frac{1}{2}}\left(\frac{zD}{h_s^2}\right)^{\frac{1}{2}}\left(\frac{h_s}{r}\right)v_K \qquad (27)$$

(compare equation 39 in Section 2). Equation (27) for the buoyant velocity leads to an estimate for the buoyant rise time t_b, compared with the Keplerian time $t_K = \Omega_K^{-1}$, of

$$\frac{t_b}{t_K} = \left(\frac{\pi}{4C_D}\right)^{-1/2}\left(\frac{\delta\rho}{\rho}\right)^{-1/2}\left(\frac{z}{D}\right)^{\frac{1}{2}}. \qquad (28)$$

If we consider this equation at a typical scale-height, $z \sim h_{\rm s}$, we see that in order for the flux tube not to be disrupted by shearing processes which occur on a Keplerian timescale, before it buoyantly rises out of the disk, we require $\delta\rho/\rho \sim 1$ and $D \sim h_s$. (This comparison may be somewhat over-restrictive since shearing instabilities for an azimuthal field grow less rapidly than for a perpendicular field.)

If the flux tube is not disrupted, its rise through the accretion disk leads to a Poynting flux of electromagnetic energy. Using our estimate of the buoyant velocity we can then determine the ratio of Poynting flux into the corona to the total generation rate of energy per unit area. First, the Poynting flux, S_z perpendicular to the disk, is given by

$$S_z \approx \frac{B^2}{4\pi}\,v_b \qquad (29)$$

$$\approx \left(\frac{\pi}{2}\right)^{\frac{1}{2}} C_D^{-1/2}\left(\frac{\delta\rho}{\rho}\right)^{\frac{1}{2}}\left(\frac{zD}{h_s^2}\right)\left(\frac{B_0^2}{4\pi P_0}\right)P_0 v_s,$$

where we have used equation (27) for the buoyant velocity and equation (10) for the scale-height and scaled the magnetic energy density by the mid-plane pressure. Two fundamental disk parameters enter this expression in the form of the product $P_0 v_s$. The central pressure P_0 can be estimated from the average disk pressure $\bar{P}$, and the α relation, viz.

$$P_0 = \frac{2}{\sqrt{\pi}}\frac{h}{h_{\rm s}}\bar{P}, \qquad (30)$$

$$\bar{P} = \alpha^{-1}(1-\eta)\frac{\dot{M}_a v_K}{4\pi r h}\left[1-\zeta(r)\right]$$

$$= \alpha^{-1}(1-\eta)\frac{\dot{M}_a v_K}{4\pi r^2}\left(\frac{h}{h_s}\right)^{-1}\left(\frac{h_s}{r}\right)^{-1}\left[1-\zeta(r)\right] \qquad (31)$$

(see equations 12 and 15).

The expression for $\bar{P}$ introduces another factor of h_s/r which is absorbed in the expression for the isothermal sound speed derived from equation (1) for the scale-height, viz.

$$v_s = \sqrt{\tfrac{1}{2}}\left(\frac{h_{\rm s}}{r}\right)v_K\left(1+\frac{B_0^2}{8\pi P_0}\right)^{-1}. \qquad (32)$$

https://doi.org/10.1071/AS99225 Published online by Cambridge University Press

Combining equations (29), (30) and (32) gives for the Poynting flux

$$S_z \approx \alpha^{-1}(1-\eta)C_D^{-1/2}\,\frac{GM\dot{M}_a}{4\pi r^3}\left(\frac{\delta\rho}{\rho}\right)^{\frac{1}{2}} \times \left(\frac{zD}{h_s^2}\right)\frac{B^2/8\pi P_0}{(1+B_0^2/8\pi P_0)^{\frac{1}{2}}}\,, \qquad (33)$$

and the ratio of Poynting flux to the rate of generation of turbulent and magnetic energy per unit area of one side of the disk [$h(\dot{\epsilon}_B+\dot{\epsilon}_{TKE})$; see equations (24) and (25)] is given by

$$f_B \approx \tfrac{2}{3}\alpha^{-1}\frac{1-\eta}{\eta}\left(\frac{\delta\rho}{\rho}\right)^{\frac{1}{2}}\left(\frac{zD}{h_s^2}\right)\frac{B^2/8\pi P_0}{(1+B_0^2/8\pi P_0)^{\frac{1}{2}}}. \qquad (34)$$

Note that the magnetic field enters in two different ways in this expression, the first through the local value B and the second through the value at the disk mid-plane B_0. It is apparent from this equation that, for say $\alpha \sim 0{\cdot}1$, $\delta\rho/\rho \sim 1$, $C_D \sim 1$, $D \sim h_s$ and $B^2/8\pi P_0 \sim 0{\cdot}1$ at $z = h_s$, the Poynting flux estimated here is an appreciable fraction of the rate of turbulent and magnetic energy generation. This gives some support to the notion that the generation of the magnetic field in the disk, followed by its transport into the corona where it is dissipated, is an attractive means of producing a hot corona. Another factor which diminishes the Poynting flux is the filling factor of such flux tubes within the disk. Clearly this has to be of order unity for buoyant transport to be important.

It must be acknowledged that the details of buoyant transport of magnetic energy are not well understood and are indeed controversial. The next section represents an attempt at understanding some of the details of magnetic transport in accretion disks.

2 Vertical Structure of Magnetic Accretion Disks

The detailed vertical structure of accretion disks, as based on the equations of vertical hydrostatic equilibrium, energy transport, opacities and equation of state, has been studied extensively in the past (e.g. Meyer & Meyer-Hofmeister 1982; Mineshige & Osaki 1983; Canizzo & Wheeler 1984; Shaviv & Wehrse 1986). It is clear that when the magnetic effects discussed in the previous section are taken into account, the disk structure must be significantly different from those derived in these studies. A large part of the accretion luminosity may not be locally dissipated, as is assumed in the α heating prescription, but rather be transported out of the main body of the disk by buoyancy.

Detailed numerical magnetohydrodynamic modelling of vertically stratified accretion disks with an isothermal or adiabatic equation of state has been performed by Stone et al. (1996). Their calculations neglected the energy transport and heating and cooling processes in the disk, and thus they could not draw any conclusions regarding the formation of a hot corona, nor compare their results to standard accretion disk models. They did find, in contrast to earlier analytical estimates and direct numerical simulations of the Parker instability (e.g. Matsumoto & Shibata 1992), that buoyant transport in their models was very ineffective. One of the motivations for the present work was to investigate the reasons underlying the discrepancy between the results of Stone et al. and the other studies.

This work attempts to bridge the gap between the standard vertical structure models and the MHD calculations by including simplified terms describing the generation, dissipation and buoyant transport of the magnetic field. Hopefully we can capture the essence of the detailed MHD result in a detailed vertical structure calculation that can model the heating and cooling processes determining the structure of the accretion disk and the associated formation of a corona.

2.1 Equations and Method

To solve for the detailed vertical disk structure we require a set of equations for the hydrostatic equilibrium, energy generation and transport, and magnetic field generation, dissipation and transport. We solve these equations treating the radiative transport in the grey two-stream approximation. The solution method is based on earlier work by Shaviv & Wehrse (1986) and Adam et al. (1988). The two-stream method approximates the full angle-dependent and frequency-dependent radiation field by considering only an ingoing and an outgoing direction, and frequency-averaged intensities. Although approximate, this method allows for a natural transition between optically thick and optically thin regions. This is not possible with the more standard way of solving the radiative transfer equation in the diffusion approximation. Our treatment of the radiative energy transport has been described in more detail in de Kool & Wickramasinghe (1999).

The inclusion of magnetic fields in the vertical structure equations is a new ingredient, so we describe the equations used in more detail. We base our work on a physical interpretation of the results of Stone et al. (1996). The simple model described below should be seen as a parametric description, based on some physical arguments that hopefully make the results scale with two parameters in a reasonable way.

It is assumed that there is a local dynamo acting in the disk that creates magnetic energy density (or

https://doi.org/10.1071/AS99225 Published online by Cambridge University Press

equivalently pressure) P_m at a rate Ω_K^{-1}. Virtually every dynamo theory predicts a growth timescale of this order (e.g. Galeev, Rosner & Vaiana 1979), so this scaling is likely to be physically correct. However, when the magnetic field becomes too strong the Balbus-Hawley (1991) instability, which performs an essential step in the dynamo mechanism by generating a radial magnetic field component from a vertical one, starts to be suppressed because the minimum wavelength of the instability λ_{BH} becomes larger than the disk thickness. We model this suppression of magnetic field generation by multiplying the linear growth rate with a correction factor

$$A(x) = 0{\cdot}74\exp[-20(x-0{\cdot}1)^3]; \quad x = \frac{P_m}{P_g}\,, \qquad (35)$$

which is numerically almost identical to the suppression factor originally derived by Tout & Pringle (1992; equation $2{\cdot}2{\cdot}3$), except that it goes to zero exponentially rather than abruptly, something we require for numerical stability. Thus the generation of the magnetic field is given by

$$\left(\frac{dP_m}{dt}\right)_{gen} = A(P_m/P_g)\Omega P_m\,. \qquad (36)$$

We assume that the dissipation (reconnection) rate scales with the typical length scale of the magnetic field variations divided by the Alfvén speed. We take the typical length scale L to be ℓh, with h the disk scale height. The dissipation rate (and magnetic heating rate H_{mag}) is then given by

$$\left(\frac{dP_m}{dt}\right)_{dis} = -\frac{\gamma v_A}{\ell h}P_m, \qquad (37)$$

where v_A is the Alfvén speed, and γ is an adjustable parameter, basically the reconnection speed divided by the Alfvén speed. Note that in this description an equilibrium between generation and dissipation is reached because the generation is suppressed, not because the dissipation increases.

Finally, an equation for the buoyant transport of magnetic field is needed. We assume that the vertical flux of magnetic energy density is given by

$$F_B = v_{eq}\Delta P_m\,, \qquad (38)$$

where ΔP_m is the typical fluctuation in the magnetic energy density that gives rise to the upward/downward motion. Here v_{eq} is the speed at which a rising or falling element moves when the buoyant forces are in equilibrium with the frictional force exerted by the surroundings, defined by

$$\rho v_{eq}^2 = \Omega^2 z\Delta\rho L\,, \qquad (39)$$

with L the typical size of an element and $\Delta\rho$ the difference in the density in the element and the mean density enforced by pressure equilibrium,

$$\Delta\rho = -\rho\frac{\Delta P_m}{P_g}\,. \qquad (40)$$

A simple consideration of the equation of motion of a rising element shows that it reaches this equilibrium speed by the time it has moved by less than its own size, so the approximation that the elements move at v_{eq} is reasonable.

Equations (38)–(40) contain the two quantities ΔP_m and ℓ, the values of which still have to be determined. To reduce the number of parameters of our model we argue that these two are related in the following way. In the turbulent disk we expect that the fluctuations in the pressure are of the order of the fluctuations in the turbulent momentum density,

$$\Delta(P_m + P_g) \sim \rho\Delta v^2\,. \qquad (41)$$

The turbulence is driven by the differential rotation, so that we can make the estimate

$$\Delta v \sim L\frac{dv_K}{dr}\,, \qquad (42)$$

with v_K the Keplerian velocity, and where it was implicitly assumed that typical sizes are the same in the radial and vertical direction. Combining these estimates, and using $h^2 \sim (c_s^2 + v_A^2)/{\Omega_K}^2$, this leads to

$$\Delta(P_m + P_g) \sim \tfrac{1}{4}\ell^2(P_m + P_g)\,, \qquad (43)$$

and we expect that roughly

$$\Delta(P_m) \sim \tfrac{1}{4}\ell^2(P_m)\,. \qquad (44)$$

Thus we are left with the parameter ℓ, the ratio of the typical size of a region with enhanced or reduced magnetic field and the disk height, which determines the effectiveness of buoyant magnetic transport

$$F_B \sim \tfrac{1}{8}\ell^{\frac{7}{2}}\Omega_K z^{\frac{1}{2}}h^{\frac{1}{2}}P_g^{-\frac{1}{2}}P_m^{\frac{3}{2}}\,. \qquad (45)$$

The numerical results of Stone et al. (1996) indicate that there is not much power in fluctuations on the larger scales comparable to the disk height, consistent with the result that they found buoyant transport to be very ineffective if we take the high power of ℓ in equation (45) into account. It is not clear, however, that the numerical diffusivity in their calculations properly models the reconnection processes that can combine smaller coherent regions of magnetic field into the larger ones for which magnetic buoyancy and escape can be important (Tout & Pringle 1992). We will therefore investigate

https://doi.org/10.1071/AS99225 Published online by Cambridge University Press

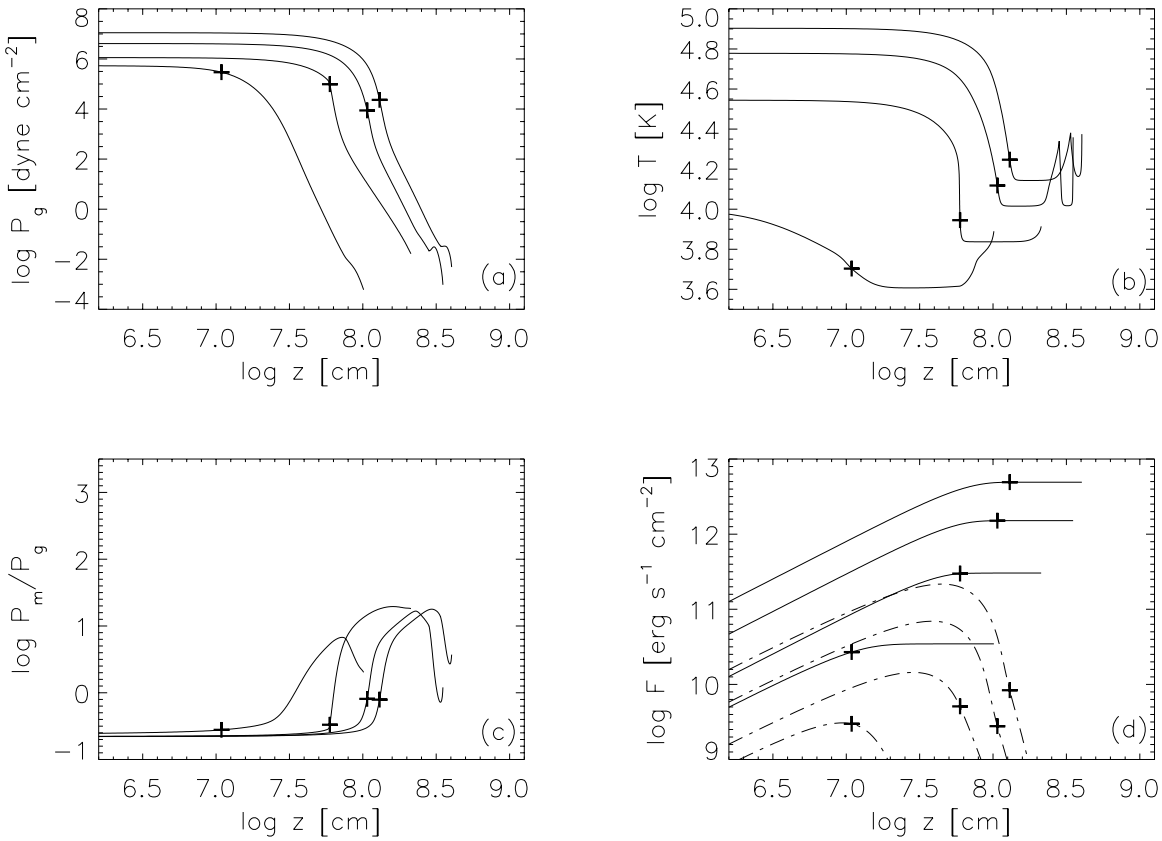

Figure 1—Vertical structure of a magnetic accretion disk with the parameters $\gamma = 0{\cdot}5$ and $\ell = 0{\cdot}5$, which is typical for the case in which buoyant magnetic energy transport is relatively inefficient. Figures 1*a* and 1*b* give the gas pressure and temperature as a function of height. Figure 1*c* gives the ratio of magnetic to gas pressure, and Figure 1*d* shows the radiative (solid) and buoyant magnetic (dashed) energy fluxes as a function of height. The crosses indicate the height where the optical depth is unity.

a range of values of ℓ that covers both effective and ineffective buoyant transport.

2.2 Results

In this section we compare the vertical structure of magnetic accretion disks with both ineffective and effective buoyant transport. The models are for an accretion disk around a $1\ M_\odot$ compact object, at a radius of 3×10^9 cm, and for four central temperatures: 10^4, $3{\cdot}5 \times 10^4$, 6×10^4 and 8×10^4 K.

Case I: Disks with predominantly local magnetic energy dissipation. As described in the previous section, our model contains the two parameters γ, the ratio of reconnection speed to Alfvén speed, and ℓ, the ratio of the size of a magnetic region and the disk height. When γ is large and ℓ small, reconnection is very efficient and most of the magnetic field is dissipated at the same place it is generated, before it has time to be transported by buoyancy effects. In Figure 1 we present a set of models where this is the case, with the parameters $\gamma = 0{\cdot}5$ and $\ell = 0{\cdot}5$.

The inefficiency of buoyant transport in this case is best demonstrated in Figure 1*d*, which compares the vertical flux in radiation with that in a buoyant magnetic field. For these parameters, the ratio of buoyant flux to radiative flux is about $0{\cdot}1$ deep inside the disk, ranging from 10^{-1} to 10^{-3} at $\tau_R = 1$ and falls to very small values at low optical depth.

In Figure 1*c*, the ratio of magnetic to thermal pressure is shown as a function of height. Deep inside the disk the dynamo mechanism regulates the magnetic pressure to be very close to the point where the wavelength of the BH instability is close to the disk height, with $P_m/P_g \sim 0{\cdot}25$. As the pressure drops, the ratio of magnetic to thermal pressure increases to a maximum of 10–20. The generation of magnetic field is completely suppressed at this point, and the buoyant flux is being used up by dissipation, which becomes quite effective now because of the high Alfvén speed. The magnetic field is dissipated so effectively that the ratio of magnetic to gas pressure actually starts to decrease again before the thermal instability point that represents our disk outer boundary is reached (de Kool & Wickramasinghe 1999). Two of the temperature profiles have a sharp maximum close to the outer edge, after which the radiative equilibrium temperature is regained once more before the thermal instability point is reached. This is caused by the sharp reduction in magnetic heating rate associated with the very sharp drop in P_m that is also evident from the decrease in P_m/P_g. This sharp reduction

https://doi.org/10.1071/AS99225 Published online by Cambridge University Press

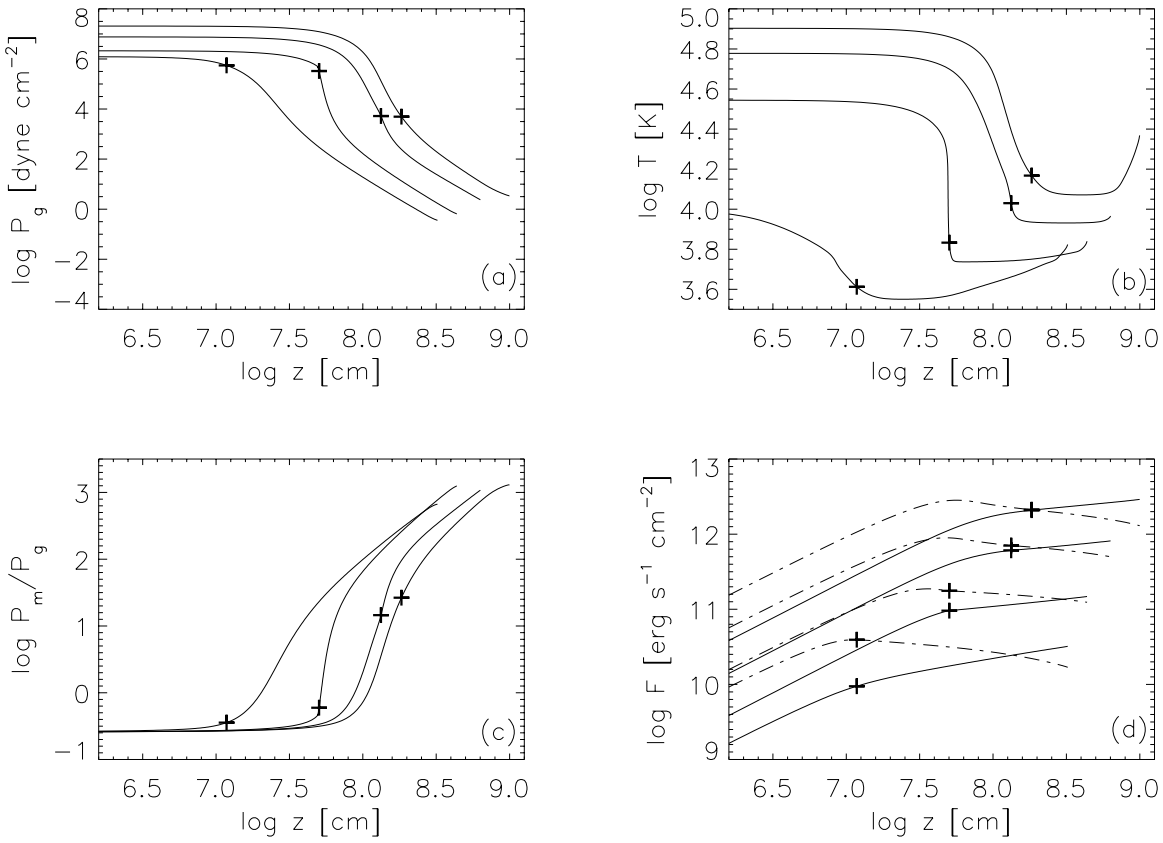

Figure 2—Vertical structure of a magnetic accretion disk with the parameters $\gamma = 0.1$ and $\ell = 0.8$, for which buoyant magnetic energy transport plays a major role.

in heating rate allows the radiative equilibrium to be regained once more.

In Figure 1*d* we see a clear trend that the maximum in the buoyant flux occurs at higher optical depth as the central temperature (or equivalently the mass flux through the disk) is increased. For the models in Figure 1, this leads to the result that for the lowest $M_\odot$ a fraction of about $0{\cdot}1$ of the total flux is generated at low optical depth, presumably in the form of optically thin line emission, even though the disk as a whole is quite optically thick. For the highest T_c model presented, this fraction is only about 10^{-3}.

Case II: Disks with efficient buoyant magnetic energy transport. In Figure 2 we present our results for the structure of disks in which buoyant magnetic energy transport plays a major role, as represented by a model with $\gamma = 0{\cdot}1$ and $\ell = 0{\cdot}8$. For these parameters, the buoyant flux deep inside the disk is about 4–6 times the radiative flux. At $\tau_R = 1$, the buoyant flux is still four times as large as the radiative flux for the lowest T_c model, and equal to the radiative flux for the highest T_c model, and in all cases the buoyant flux is still significant at the thermal instability point. The ratio of magnetic to gas pressure increases outwards as far as we can calculate, resulting in quite extended outer layers. In all cases, but especially the low T_c one, there is very significant dissipation in the optically thin, but still relatively cool, outer layers of the disk. The trend that the maximum in the buoyant flux occurs at higher optical depth as the mass flux through the disk is increased is even more obvious here than in Figure 1.

A fraction of $0{\cdot}25$–$0{\cdot}5$ of the energy generated in the disk escapes past the thermal instability point, and will either escape to infinity in the form of Poynting flux, or will be dissipated beyond the instability point giving rise to a hot corona. However, our results show that this hot corona cannot be in hydrostatic and thermal equilibrium and that dynamical effects such as outflows must become important [see Meyer & Meyer-Hofmeister (1994) for a study of such an outflowing corona.]

2.3 Conclusions

The models indicate that buoyant magnetic transport can only be important if the magnetically over- and under-pressured regions have a size comparable to the disk scale height, and if the perturbation of the magnetic field is a significant fraction of the total pressure. Otherwise, their rise time is so long that reconnection, even at a small fraction of the Alfvén speed, will dissipate the magnetic field before it can emerge. The hydromagnetic turbulence developing in the numerical MHD calculations of Stone et al. (1996) does not form such large coherent regions, and therefore these do not show significant buoyancy effects.

https://doi.org/10.1071/AS99225 Published online by Cambridge University Press

References

Adam, J., et al. 1988, A & A, 183, L1
Balbus, S. A., & Hawley, J. F. 1991, ApJ, 376, 214
Canizzo, J. K., & Wheeler, J. C. 1984, ApJS, 40, 1
de Kool, M., & Wickramasinghe, D. L. 1999, MNRAS, 307, 449
Galeev, A. A., Rosner, R., & Vaiana, G. S. 1979, ApJ, 229, 318
Haardt, F., & Maraschi, L. 1997, ApJ, 476, 620
Kuncic, Z., & Bicknell, G. V. 1999, in preparation
Matsumoto, R., & Shibata, K. 1992, PASJ, 44, 167
Meyer, F., & Meyer-Hofmeister, E. 1982, A & A, 106, 34
Meyer, F., & Meyer-Hofmeister, E. 1994, A & A, 288, 175
Mineshige, S., & Osaki, Y. 1983, PASJ, 35, 377
Shakura, N. I., & Sunyaev, R. 1973, A & A, 24, 337
Shaviv, G., & Wehrse, R. 1986, A & A, 159, L5
Stone, J. M., et al. 1996, ApJ, 463, 656
Tout, C. A., & Pringle, J. E. 1992, MNRAS, 259, 604

https://doi.org/10.1071/AS99225 Published online by Cambridge University Press